



Modelling of urban ambient N, N-dimethylformamide concentrations in a small-scale synthetic leather industrial zone*

Yu-mei WEI^{1,2}, Wei-li TIAN^{1,2}, Ying-yue ZHENG^{1,2}, Qing-yu ZHANG^{†‡1,2},
 Lei JIANG^{1,2}, Zu-cheng WU¹

⁽¹⁾Department of Environmental Engineering, Zhejiang University, Hangzhou 310027, China

⁽²⁾Zhejiang Provincial Engineering Research Center of Industrial Boiler & Furnace Flue Gas Pollution Control, Hangzhou 311202, China

[†]E-mail: qy_zhang@zju.edu.cn

Received June 27, 2010; Revision accepted Dec. 2, 2010; Crosschecked Apr. 21, 2011

Abstract: A method to model small-scale ambient concentrations of N, N-dimethylformamide (DMF) in a synthetic leather industrial zone was developed. Longwan, a district of Wenzhou City in Southeast China, was selected as the study area. DMF emissions at the synthetic leather industrial zone were inventoried, during 2007, and an AMS/EPA regulatory model (AERMOD) was used to simulate DMF concentrations using 10000 100 m×100 m grids for the 2006 period. In 2007, actual DMF concentrations were recorded at seven DMF monitoring stations, and were compared with simulated results for the same timeframe. Simulated DMF concentrations were predicted to be in the range of 0.012–2.31 mg/m³, which is similar to the range of the monitored dataset results. A large majority (93%) of relative errors (REs) between simulated and monitored concentrations ranged from 0.48% to 189.4%. While DMF emissions within factories did not exceed the regulated emission limit, simulations indicated that, in 2006, 20% of the daily average ambient DMF concentrations exceeded this limit. This Modelling method could be applied in evaluating regional atmospheric environmental capacities and human exposure to DMF.

Key words: N, N-dimethylformamide (DMF), Geographic information system (GIS), Emission inventory, AERMOD, Small-scale
doi:10.1631/jzus.A1010245 **Document code:** A **CLC number:** X51

1 Introduction

N, N-dimethylformamide (DMF) has complete miscibility in water and most organic solvents, and hence it has a broad industrial application for the production of synthetic leather, polyurethane resin, orlon, etc. (Howard, 1993; Environment Canada, 1998). However, overexposure of humans to DMF has been associated with hepatotoxicity, alcohol intolerance, possible embryotoxicity, and teratogenicity (Calvert *et al.*, 1990; Hansen and Meyer, 1990). In the USA and China, the regulated air exposure concen-

tration limits for DMF emissions are 30 and 10 mg/m³, respectively, in the workplace (MHPRC, 1979; Jilin Library, 1984). While DMF emission levels for a particular synthetic leather factory may remain within the regulated limit at industrial zone aggregations ambient (i.e., outside of the workplace), DMF concentrations may in fact exceed the regulated workplace concentration limit as a result of accumulative DMF emissions of several factories (Zhang, 2007). Hence, pollution caused by overall DMF emissions continues to be a serious public concern.

The total amount of DMF emissions within industrial zones should be subject to regulation. The environmental capacity is the maximum permitted pollution load that may be discharged into the atmosphere without violating the desired air quality of regional planning objectives (Krishna *et al.*, 2004). This value can be used to determine the maximum

[†] Corresponding author

* Project (No. 200809103) supported by the "State Environmental Protection Commonwealth Trade Scientific Research" Project of Ministry of Environmental Protection of China

© Zhejiang University and Springer-Verlag Berlin Heidelberg 2011

permitted emission of certain pollutants in an area, and to set the emission quota of each factory within the area accordingly. To date, the total emission control, which is based on the environmental capacity, has been used widely in China to mitigate air pollution (Yang *et al.*, 1999).

Currently, two methods are used to estimate environmental capacity, namely the *A-P* value method and multi-source model method (Fang *et al.*, 2008). The *A-P* value method calculates the environmental capacity primarily using the size of the study area, but does not take into account meteorological and topographic data. On the other hand, the multi-source model method uses air pollutant dispersion models to calculate environmental capacity. Such dispersion models usually consider detailed emission inventories, emission sources distribution, meteorological and topographic data, and other associated datasets. Hence, while the *A-P* value method generates an ideal environmental capacity value, the multi-source model method is more likely to correspond to the actual situation (Fang *et al.*, 2008). Therefore, when setting regulation limits in an area, the value based on the results of the *A-P* method may indicate pollutant concentrations exceeding the limits at some sites, while the multi-source model method may provide a more realistic inference (An *et al.*, 2007; Fang *et al.*, 2008).

Air dispersion models have the ability to simulate geographic information system (GIS) based pollutant concentrations using fine-scale receptor grids (Lin and Lin, 2002). Such models have been used for a range of situations, such as human exposure risk assessments and environmental capacity evaluation (Zhou *et al.*, 2003; Krishna *et al.*, 2004; Goyal *et al.*, 2006; Silverman *et al.*, 2007; Özkaynak *et al.*, 2008). In most studies, pollutant concentrations have been simulated with 1 km×1 km receptor grids (Zhang *et al.*, 2008). However, for industrial zones where the spatial scale is small, pollutant emissions are likely to vary within a narrow range. In order to obtain detailed air pollutant dispersion concentrations, it is therefore necessary to reduce simulated receptor grids to 500 m×500 m, or as much as 100 m×100 m. Information with respect to factory location and respective emission rates is important to calculate air pollutant emission inventories for application to air dispersion models (Samaali *et al.*, 2007). Furthermore, the

emission quota of each factory may also be allocated according to the environmental capacity based on the emission inventories (SEPA, 2003). These combined parameters may prove significant for environment capacity evaluation and pollution mitigation. Hence, there is an urgent requirement to establish emission inventories based on GIS and simulated air pollutant dispersion distributions, particularly for small-scale industrial zones.

In this paper, we first established a GIS based DMF emission inventory using the case study of the synthetic leather industrial zone of Longwan, a district of Wenzhou City in Southeast China. The AMS/EPA regulatory model (AERMOD) was used to evaluate the ambient DMF concentrations of this district. We set up seven DMF monitoring stations to record DMF concentrations in the air of Longwan for four days in 2007: 28–29 March and 9–10 July. We compared and verified the model simulation results with those obtained from monitoring datasets. Finally, we presented simulations of ambient DMF concentrations to estimate the environmental capacity of Longwan during 2006, using 10000 grids of 100 m×100 m. The results were considered with respect to the potential impact on the human population residing in this region.

2 Study area

The Longwan District, located on the south coast of East China Sea, is one of the three major urban areas of Wenzhou city in Zhejiang Province (Fig. 1). The urban area of Longwan covers 279 km² with a population of 306000. The prevailing wind direction is north-north-east. The climate of Longwan is humid subtropical maritime, with an annual average temperature of 14–18 °C and annual average rainfall of 1500–1800 mm.

The Longwan synthetic leather industrial zone covers 1.13 km². The first synthetic leather factory in Longwan was built in the 1990s. Today, the district has 84 synthetic leather factories, including 30 polyvinylchloride (PVC) synthetic leather factories with 42 production lines, and 54 polyurea-formaldehyde (PU) synthetic leather factories with 260 production lines. Longwan is the largest synthetic leather production zone worldwide, producing about 70% of

China's synthetic leather goods and 50% worldwide. In recent years, control measures have been introduced to regulate DMF emissions.



Fig. 1 A map of the Longwan District (pentacle) in Wenzhou City, Zhejiang Province, China

3 Methodology

3.1 DMF in the manufacturing process of synthetic leather

Synthetic leather manufacturing processes are mainly classified as wet and dry processes based on how solvents are expelled from the products (Wang *et al.*, 2006). Fig. 2 illustrates the process of wet and dry operations for the manufacturing of synthetic leather at the Longwan industrial zone (Wang *et al.*, 2006).

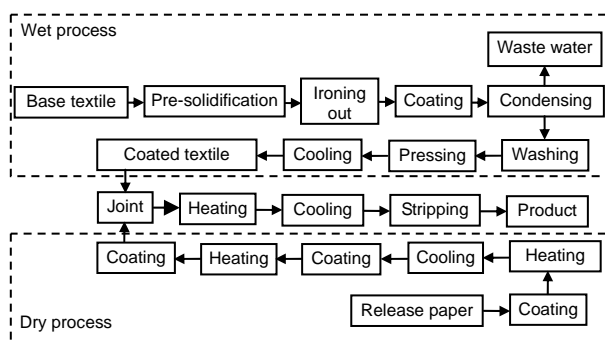


Fig. 2 Flow diagram of the steps of operation for wet and dry synthetic leather manufacturing processes

In the wet process, PU resin is dissolved in organic solvents (DMF). The base textile is dipped into material for pre-solidification, ironing out to dry, coating, condensing in the condensation tank, washing in water to remove residual DMF, and finally

drying and cooling to room temperature. In the dry process, PU resin is dissolved in organic solvents (DMF, methyl ethyl ketone (MEK), and toluene). The release paper is coated and subsequently heated in an oven to remove the solvents. The release paper is then adhered to the coated base textile of the wet process. It is dried again and cooled to room temperature. During the condensing phase of the wet process, wastewater contains 20% DMF. Wastewater is usually disposed for rectification, and most DMF is recycled.

Based on our investigation, DMF consumption, the emission, and recycling of one production line were almost the same for all synthetic leather factories in the study area. Therefore, we would take a production line as an example for DMF emission calculation.

3.2 DMF consumption in the synthetic leather industry

The amount of PU resin used in a production line of synthetic leather factories can be calculated according to the formulas:

$$Q_T = M_T r_T + S_T, \quad (1)$$

$$M_T = N_T V_T T, \quad (2)$$

where Q is the total DMF consumption (kg); M is the resin consumption (kg); r is the percentage of DMF content of resin; S is the DMF consumption as a solvent (kg); N is the resin consumption per meter of base textile (wet process) or release paper (dry process) (kg/m); V is the velocity of base textile (wet process) or release paper (dry process) (m/h); T is the operating time of the factory (h); I is type of production (wet or dry process).

In the wet process, resin consumption of base textile is about 0.378 kg/m, and base textile velocity is about 840–900 m/h. However, in the dry process, resin consumption of release paper is about 0.16–0.17 kg/m, while release paper velocity remains at 840–900 m/h. The operating time of synthetic leather factories in the study area is about 210 d/yr, i.e., 5040 h/yr.

Furthermore, the proportion of DMF used in resin and solvent for the wet process differs to that for the dry process. In the wet process, 700 kg of raw DMF material is used per 10^3 kg of resin, with a further 700 kg of DMF being added as the solvent.

However, in the dry process, 500 kg of raw DMF material is used per 10^3 kg of resin, with a further 500 kg of DMF being added as the solvent.

3.3 DMF emissions in the manufacturing process

DMF emissions are estimated based on the mass balance of the manufacturing process according to the total DMF consumption. This method calculates pollutant emission into the environment using the difference between all inputs and measurable outputs of the system (Coufal *et al.*, 2006). DMF emissions were calculated based on the following formulas:

$$Q_E = Q_{W-F} + Q_{W-E} + Q_{D-F} + Q_{D-E} + Q_{R-E}, \quad (3)$$

$$Q_{W-T} = Q_{W-F} + Q_{W-E} + Q_{W-W}, \quad (4)$$

$$Q_{D-T} = Q_{D-F} + Q_{D-C}, \quad (5)$$

$$Q_{D-E} = Q_{D-C} \cdot (1 - \eta), \quad (6)$$

$$Q_{R-E} = Q_{R-IN} - Q_{R-T} - Q_{R-B} - Q_{R-C} - Q_{R-O} - Q_{R-D}, \quad (7)$$

where Q_E is the total DMF emission (kg); Q_{W-F} and Q_{W-E} are the fugitive and organized emissions of DMF in the wet process respectively (kg); Q_{D-F} and Q_{D-E} are the fugitive and organized emissions of DMF in the dry process respectively (kg); Q_{R-E} is the DMF emission in the rectification process (kg); Q_{W-T} and Q_{D-T} are the total DMF consumptions in the wet and dry processes respectively (kg); Q_{W-W} is the DMF contained in wastewater (kg); Q_{D-C} is the DMF collected by control facilities (absorption column) (kg); η is the percentage efficiency of control facility; Q_{R-IN} is the total DMF collected for recycling (kg); Q_{R-T} and Q_{R-B} are the DMF contained in the water at the top and bottom of the rectification column, respectively (kg); Q_{R-C} is the DMF contained in the circulating water pool (kg); Q_{R-O} is the recycled DMF (kg); Q_{R-D} is the DMF decomposition (calculated by dimethylamine produced) (kg).

The DMF emissions during the ironing out process are collected in the chimney stack prior to emission, resulting in organized emissions into the atmosphere. According to the monitoring data of 54 PU synthetic leather factories, organized DMF emission in the wet process from the chimney stack is estimated to be 4.2×10^3 kg/yr per production line. The DMF fugitive emission for other processes in wet production, such as pre-solidification, coating, and condensing, is estimated to be 1.039×10^5 kg/yr per production line. In the dry process, 6.631×10^5 kg/yr

of DMF per production line is collected for disposal in the absorption column, and the disposal efficiency is estimated at 99%. Therefore, the organized emission of DMF after absorption is estimated to be 6.63×10^3 kg/yr per production line. According to the monitoring data, fugitive emissions of DMF, which were not collected but volatilized in the process of dissolving, coating, and heating, are estimated to be 5.686×10^4 kg/yr per production line.

The total DMF collected for recycling is 2.052×10^6 kg/yr per production line. DMF contained in each unit of operation is calculated based on water fluxes and DMF concentrations. According to the metering instrument data of 11 factories, the wastewater fluxes in the top rectification column, the bottom rectification column, and circulating water pool are approximately 2×10^3 – 7×10^3 , 100–300, and 6×10^3 – 8×10^3 kg/h, respectively. The recycling flux of DMF is 1.1×10^3 – 2.8×10^3 kg/h. At 11 factories, we collected water samples of each unit of operation to test DMF concentrations.

3.4 AERMOD

AERMOD is a near field steady state Gaussian air pollutant dispersion model proposed by the US EPA (US EPA, 2004a; Cimorelli *et al.*, 2005; Perry *et al.*, 2005). The model aims to simulate short-range dispersion (up to 50 km) from multiple sources of different emission types including point, area, and volume sources. Previous studies have focused on the performance of AERMOD since it was developed. The accuracy and reliability of results of AERMOD at different spatial scales in urban areas have been evaluated in comparison to other dispersion models using 17 field-study databases (Perry *et al.*, 2005). Perry *et al.* (2005) found that with few exceptions, AERMOD's performance is superior to those of other applied models.

In this study, AERMOD was used to simulate annual and daily average concentrations of DMF. The model input data included source location and parameter data, meteorological data, terrain data, and receptor locations. As the study area is a coastal plain with the flat terrain, the simulation has been carried out using a flat option.

3.4.1 Source location and parameter data

DMF emissions were divided into two sources,

point and area. We considered point sources to be organized sources (i.e., emissions from chimney stacks ≤ 15 m), while emissions from factory workshops were considered to be area sources. In the study area, there were 75 point sources and 54 area sources in total.

Point source characteristics include source location, pollutant emission rate, release height above ground, stack inside diameter, and stack gas exit temperature and exit velocity. Information on each point source was compiled, such as stack height and diameter, as well as emission exit velocity and exit temperature. The latitude and longitude of each point source was measured using a handheld global positioning system (GPS). The DMF emission rate was calculated by dividing the average running time of 54 control factory facilities against DMF emissions. In this study, we did not list the specific information of each point, but gave the range of each parameter of 75 point sources. Based on the investigation, the point source stack height and the diameter were approximately 16–25 and 0.8–1.2 m, respectively, and the emission exit velocities from point sources ranged from 15.92–21.23 m/s, while the exit temperature was 25–40 °C.

Area source inputs include source location, area emission rate, lengths of X and Y side of the area, orientation angle for the rectangular area in degrees from North, and release height above ground. The workshops of each factory were identified as the area sources. For area sources, emissions were distributed with respect to the wet and dry production lines of each workshop. The latitude and longitude of the four corners of each workshop in all 54 factories were measured using a handheld GPS. Information on length and width of each workshop was compiled. The orientation angles for the rectangular area sources in degrees from North were calculated, and are shown in Fig. 3. The wet and dry production lines are usually located in the first and second floors of the workshop. Therefore, the average DMF emission height of area sources is 3 or 6 m based on the height of the corresponding floor.

3.4.2 Meteorological data

To develop meteorological inputs for AERMOD, the AERMET meteorological processor was used to calculate hourly boundary layer parameters such as

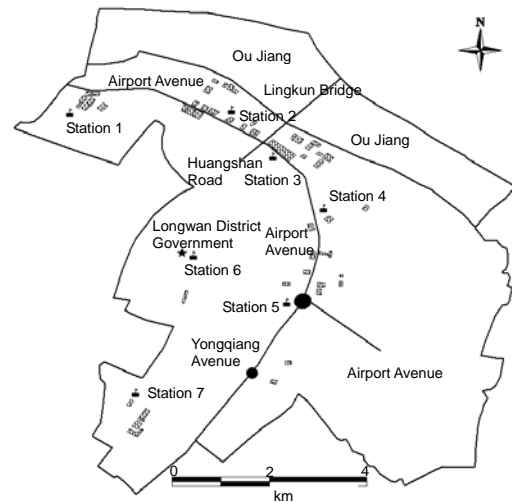


Fig. 3 Angle of orientation for 54 rectangular workshops and seven monitoring stations in the Longwan District of Wenzhou City, China

the Monin-Obukhov length, temperature scale, convective velocity scale, and sensible heat flux. AERMET requires the input of surface characteristics in combination with standard meteorological observations. In the absence of meteorological observations at an hourly interval, we used the Fifth-Generation NCAR/Penn State Mesoscale Model (MM5) to calculate these meteorological data, according to the latitude and longitude coordinates of Longwan. MM5 was developed by Pennsylvania State University and the National Centre for Atmospheric Research in Boulder, Colorado, USA (Grell *et al.*, 1995). It has been widely used and tested to derive meteorological inputs for air dispersion models (Sokhi *et al.*, 2006; Han, 2007; Matthias *et al.*, 2008). In order to validate the simulation results of MM5, we compared the simulated meteorological data with meteorological data from a nearby station (Wenzhou Station: 58659). Air temperature, wind speed, and wind direction were statistically analyzed due to their known significant influence on DMF dispersion (Horan and Finn, 2008; Klepeis *et al.*, 2009). Surface and profile meteorological inputs for AERMOD are listed in Table 1. The necessary meteorological data calculated by MM5 are listed in Table 2.

3.4.3 Surface characteristic

Surface characteristics (surface roughness, Bowen ratio, and albedo) are also required AERMET

Table 1 Meteorological inputs for AERMOD

No.	Surface meteorological input	No.	Surface meteorological input	No.	Profile meteorological input
1	Sensible heat flux (W/m ²)	10	Height ³ (m)	1	Height (m)
2	Friction velocity (m/s)	11	Temperature (K)	2	Top*
3	Convective velocity scale (m/s)	12	Height ⁴ (m)	3	Wind direction (°)
4	Vertical potential temperature gradient (K/m)	13	Precipitation code	4	Wind speed (m/s)
5	Height ¹ (m)	14	Precipitation rate (mm/hr)	5	Temperature (K)
6	Height ² (m)	15	Relative humidity (%)	6	Initial lateral plume size (m)
7	Monin-Obukhov length (m)	16	Station pressure (hPa)	7	Initial vertical plume size (m)
8	Wind speed (m/s)	17	Cloud cover (tenths)		
9	Wind direction (°)				

¹ Height of the convectively-generated boundary layer; ² Height of the mechanically-generated boundary layer; ³ Height above which the wind was measured; ⁴ Height above which the temperature was measured; * top=1, if this is the last (highest) level, and otherwise 0

Table 2 Meteorological data calculated by MM5

12-h upper meteorological data	24-h surface meteorological data
Wind speed (m/s)	Wind speed (m/s)
Wind direction (°)	Wind direction (°)
Temperature (K)	Temperature (K)
Pressure (hPa)	Cloud cover (tenths)
Height (m)	
Relative humidity (%)	

inputs to calculate planetary boundary layer (PBL) parameters. EPA has released a computer program (AERSURFACE) to calculate these values from the US Geological Survey (USGS) National Land Cover Data 1992 archives (NLCD92) (US EPA, 2008). As the NLCD92 data is not available for the study area, we calculated these values based on the method recommended by ADEC, which has also been used by Trinity Consultants (USA) (ADEC, 2009). According to EPA's stated guidance, the applicable sectors for calculating surface roughness, Bowen ratio, and albedo were determined (US EPA, 2004b). The land classification for the study area was determined using a land-use map of Longwan and site visits. Then, the fraction of each land classification and the distance between the meteorological site and the centroid of each classification were estimated. The above values were referenced in a table, along with the seasonal surface roughness, Bowen ratio, or albedo (as applicable) associated with each classification (US EPA, 2004b). Surface roughness was calculated by weighting each applicable value by land fraction divided by the distance. Bowen ratio and albedo were

calculated by weighting each applicable value by land fraction. The land of the study area can be classified as indicated in Table 3.

Table 3 Fraction of land classification of the study area

Land cover category	Area (km ²)	Fraction of total area
Open water	22	0.22
Low intensity residential	8	0.08
Commercial/Industrial/Transportation	31	0.31
Evergreen forest	12	0.12
Urban/Recreational grasses	4	0.04
Row crops	23	0.23
Total	100	1

The study area is a coastal plain with the flat terrain and dense river network. As shown in Table 3, commercial, industrial, and transportation lands account for the largest proportion of the total area. Owing that the area with dense river network is close to Oujiang River, the land use of open water accounts for 22% of the total area. Longwan is the suburb district of Wenzhou City, and about 8% area is of low residential density.

3.4.4 Receptor locations

In small-scale regions, air pollutant concentrations may vary obviously across the area (Spicer *et al.*, 1996). Therefore, high resolution receptor grids are necessary to obtain detailed pollutant concentrations. Hence, we simulated DMF concentration distribution using the receptor grids of 100 m×100 m. All receptors were identified by their coordinates.

3.5 DMF ambient concentration monitoring

In order to verify DMF emission inventories to simulate the concentration distribution by the dispersion model, seven monitoring stations representing different urban communities within the study area were characterized. The monitoring sites were located in industrial (Stations 2, 3, 7), residential (Stations 1, 4), and commercial zones (Station 6), as well as along major roads (Station 5) (Fig. 3). We obtained information from Wenzhou Environment Monitoring Center, which recorded DMF concentrations according to national monitoring standard (MEP-GAQSIQ, 2008). The study occurred in the spring and summer seasons (March and July), which is the midseason of synthetic leather production. During this period, most factories in the study area are operating. Therefore, at each monitoring site, samples were collected hourly at 10:00, 11:00, 12:00, and 13:00, during 28–29 March and 9–10 July, 2007. The production of all 54 synthetic leather factories were also investigated during the periods of monitoring. The relative errors (REs) between the monitored and simulated data were evaluated using the following formula:

$$RE = \frac{|C - C_0|}{C} \times 100\%, \quad (8)$$

where C represents the monitored data, and C_0 represents the simulated data.

4 Results and discussion

4.1 DMF emissions of synthetic leather production

As it is shown in Table 4, total estimated consumptions of DMF in wet and dry processes for one production line were 2.24×10^6 and 0.72×10^6 kg/yr, accounting for 76% and 24% of total consumption respectively. For 54 synthetic leather factories in the study area, there were 139 wet and 121 dry production lines in total. Hence, the total consumption of DMF in the study area reached 3.98×10^8 kg/yr.

The test results of water samples at 11 factories showed that DMF concentrations in water at the top and bottom rectification columns and circulating water pools were approximately 0.06–2.35, 36.12–90.73, and 0.13–0.94 mg/ml, respectively. In addition,

the dimethylamine concentrations in water at the top and bottom rectification columns and circulating water pools were approximately 0.53–2.53, 0.01–1.31, and 0.5–1.2 mg/ml, respectively.

Table 4 DMF consumption of a representative synthetic leather factory in the wet and dry processes

Type of DMF consumption	DMF consumption of one production line ($\times 10^3$, kg/yr)	
	Wet process	Dry process
DMF used in resin	1120	360
DMF used as solvent	1120	360
Total	2240	720

Table 5 showed the estimated amount of DMF emissions from the chimney stack, workshop area, and recovery process of one production line. DMF emissions in one wet and one dry production lines were 1.081×10^5 and 6.35×10^4 kg/yr, accounting for 63% and 37% of total emissions, respectively. Fugitive emission from workshop was 1.608×10^5 kg/yr and accounted for 94% of total emissions. The part of DMF emitted at a low height has a greater impact on human health, and hence mitigation measures should be focused on DMF emissions from workshops. According to total production lines, total emission of DMF in the study area was 2.27×10^7 kg/yr.

Table 5 DMF emissions from the chimney stack, workshop area and recovery process

Emission source	DMF emissions of one production line ($\times 10^3$, kg/yr)		
	Wet line	Dry line	Total
Stack	4.2	6.63	10.83
Workshop	103.9	56.86	160.76
Recovery process	0.033	0.01	0.043
Total	108.133	63.5	171.633

4.2 Comparison of simulated and monitored meteorological data

Fig. 4 showed the comparison of simulated meteorological data with those of monitored meteorological data during 23–29 March and 4–10 July, 2007, which encompassed the days that the synthetic leather factories were monitored. The simulated data of the three meteorological parameters closely resembled the monitored data.

Table 6 presented an index of agreement (IOA), root mean square error (RMSE), and mean bias error (MBE) of three of the meteorological parameters (air

temperature, wind speed, and wind direction) (Willmott, 1981; Gunhan *et al.*, 2005; Zawar-Reza *et al.*, 2005). As shown in the table, the simulated air temperature closely resembled the monitored datasets, with the IOA, RMSE, and MBE being 0.98, 1.7, and -1.3 , respectively. The IOA, RMSE, and MBE of wind speed were 0.84, 0.1, and 0.1, respectively, and those of wind direction were 0.83, 63.2, and 14.0, respectively. The IOA of these three meteorological parameters were greater than 0.8, with values above 0.6 being accepted as representative (Titov *et al.*, 2007). However, RMSE and MBE of wind direction were much larger than those of other two parameters. Therefore, MM5 simulations performed best for temperature, followed by wind speed and wind direction.

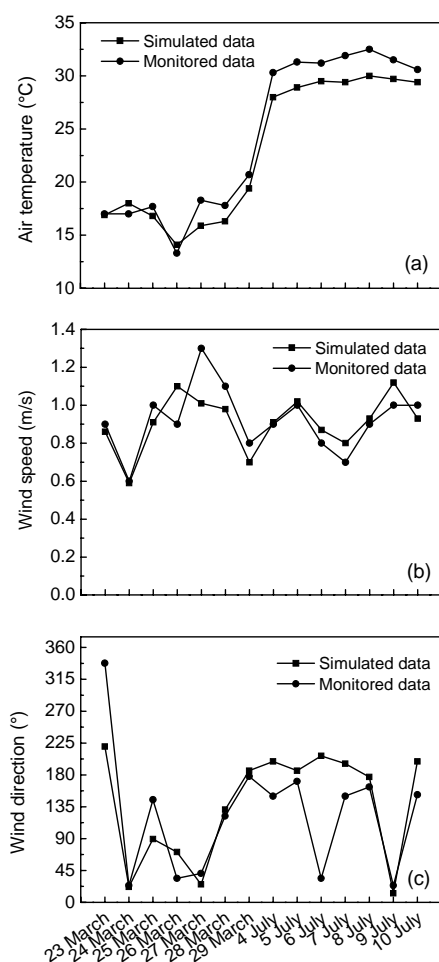


Fig. 4 Curves of air temperature (a), wind speed (b), and wind direction (c) in the Longwan District of Wenzhou City, China during 23–29 March and 4–10 July 2007

Table 6 Comparison of three meteorological parameters (air temperature, wind speed, and wind direction) during 23–29 March and 4–10 July 2007

Meteorological parameter	IOA	RMSE	MBE
Air temperature (°C)	0.98	1.7	-1.3
Wind speed (m/s)	0.84	0.1	0.1
Wind direction (°)	0.83	63.2	14.0

IOA: index of agreement; RMSE: root mean square error; MBE: mean bias error

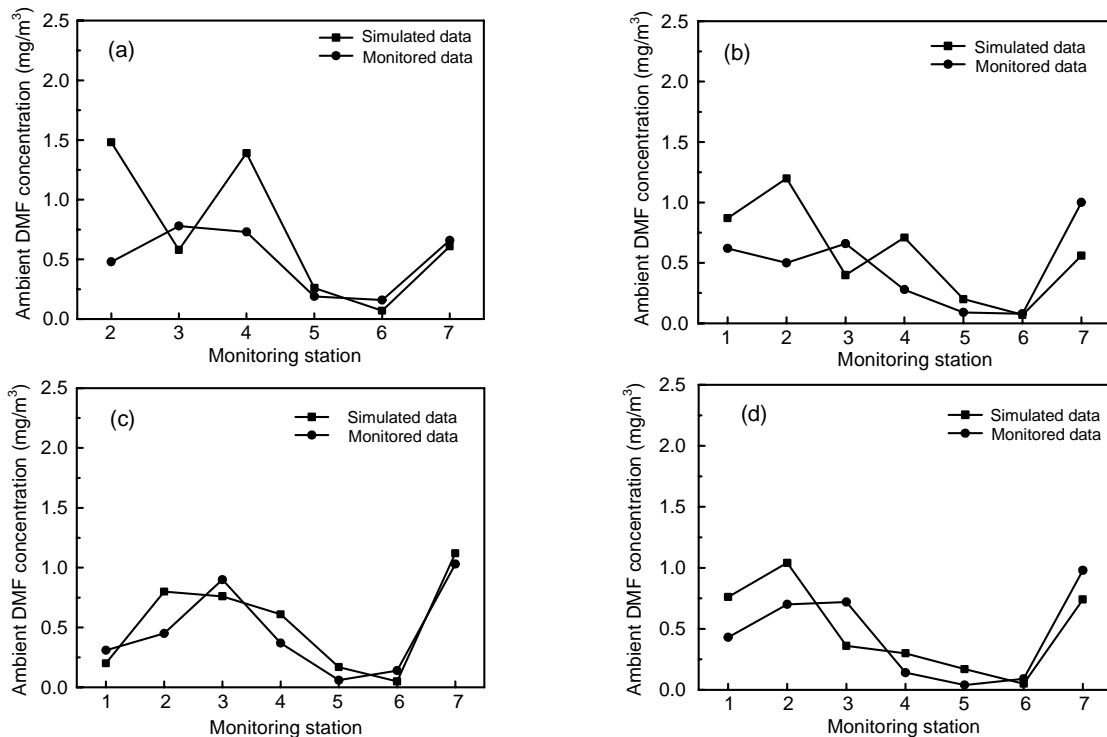
4.3 Comparison of simulated and monitored DMF concentrations

The wind speed and wind direction during the monitoring period were shown in Table 7. The results of simulated and monitored DMF concentrations at each monitoring station during 28–29 March and 9–10 July, 2007, were shown in Figs. 5–8.

On 28 March 2007 (Fig. 5), the REs between the monitored and simulated data of Stations 2 and 4 were greatest between 10:00 and 11:00 (207.8% and 89.8%, respectively). The same two stations also exhibited their greatest discrepancy between 11:00 and 12:00 (140.8% and 152.5%, respectively). However, between 12:00 and 13:00 and between 13:00 and 14:00, the REs between simulated and monitored data were the greatest at Station 5 (81.6% and 314.6%, respectively), while those for all other stations remained below 100% during these survey periods. Overall, REs between simulated and monitored data less than 50% were obtained for seven stations during 13 of the 28 survey hours (i.e., 7 stations \times 4 hours per station), which accounted for 46% of the total monitoring points. Overall, REs in excess of 200% were obtained for two of the surveyed hours, which accounted for 7% of the total monitoring points. Comparatively, the REs between simulated and monitored data of Stations 2 and 4 were larger than those of the other stations. In fact, the simulated DMF concentrations exceeded monitored concentrations for these two stations. These discrepancies could be attributed to the locations of the two stations and meteorological conditions during the monitoring periods. For example, Station 2 was located to the west of the synthetic leather industrial zone, and surrounded by more than 10 factories (three factories to the northwest, three to the west, and four to the south of the station). Station 4 was located to the east of the

Table 7 Wind speed and wind direction during 28–29 March and 9–10 July, 2007

Monitoring period		Wind speed (m/s)	Wind direction	Monitoring period		Wind speed (m/s)	Wind direction
28 March	10:00–11:00	1.6	SW	9 July	10:00–11:00	1.6	N
	11:00–12:00	1.6	SW		11:00–12:00	1.6	N
	12:00–13:00	1.1	SW		12:00–13:00	1	N
	13:00–14:00	1.1	SW		13:00–14:00	1	N
29 March	10:00–11:00	1.5	S	10 July	10:00–11:00	1.8	S
	11:00–12:00	1.5	S		11:00–12:00	1.8	S
	12:00–13:00	1.5	S		12:00–13:00	1.3	S
	13:00–14:00	1	S		13:00–14:00	0.7	S

**Fig. 5** Ambient DMF concentration for 28 March 2007 at 10:00–11:00 (a), 11:00–12:00 (b), 12:00–13:00 (c), and 13:00–14:00 (d)

The monitored DMF concentration at Station 1 at 10:00–11:00 on 28 March was missing due to the device malfunction

synthetic leather industrial zone, and surrounded by three factories (one factory to the east and two to the south of the station). Monitoring concentrations of these two stations would be affected by factories to their south and west due to the southwest wind direction. On this day of monitoring, not all factories in the vicinity of these two stations may have been operating, which resulted in lower concentrations of monitored DMF in comparison to simulated ones. Moreover, according to the meteorological data on 28 March 2007, wind speed between 10:00 and 12:00 (1.6 m/s) was higher than other survey periods (1.1 m/s), which also resulted in a lower monitored DMF concentration.

On 29 March 2007 (Fig. 6), the REs between simulated and monitored data were below 100% between 10:00 and 14:00 for all stations expect for Station 2. The RE for Station 2 was 914.1% between 11:00 and 12:00. The REs between simulated and monitored data were below 50% at seven stations for 20 of the survey hours, accounting for 71% of the total monitoring points. An RE in excess of 200% was recorded for one station only during one hour, accounting for 4% of total monitoring points. On this day of monitoring, a synchronous discharge of nearby synthetic leather factories may have resulted in monitored DMF concentrations being higher than those of simulated concentrations for several stations.

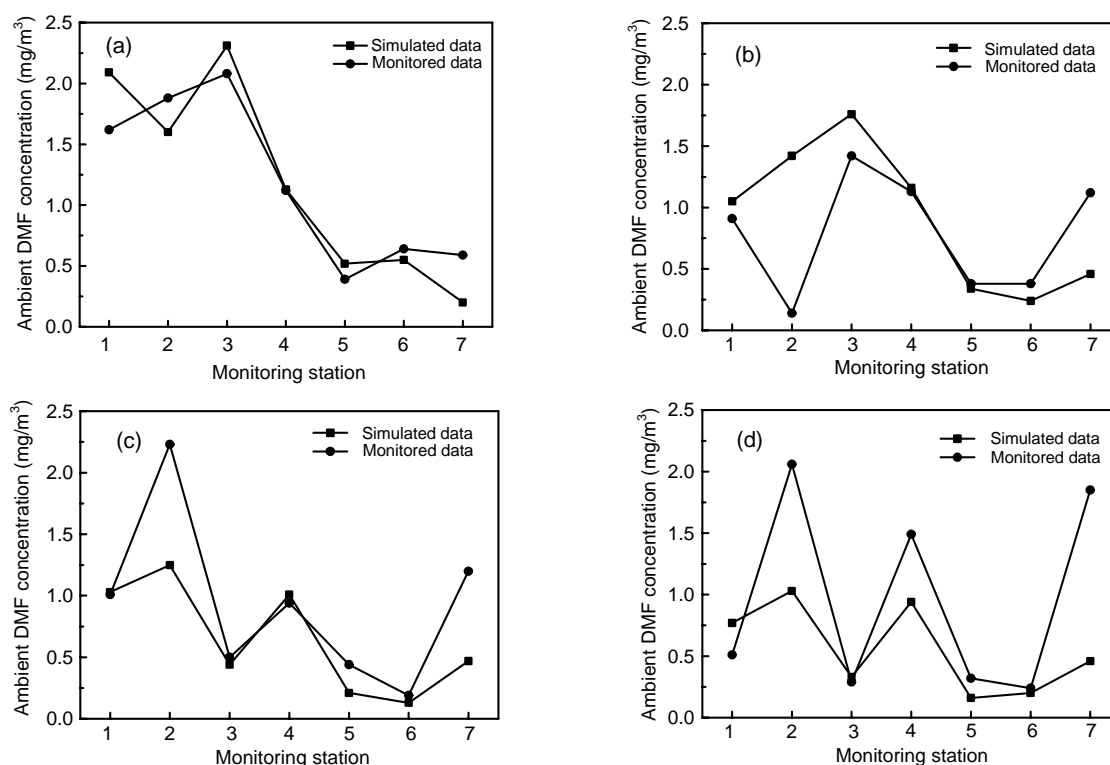


Fig. 6 Ambient DMF concentration for 29 March 2007 at 10:00–11:00 (a), 11:00–12:00 (b), 12:00–13:00 (c), and 13:00–14:00 (d)

On 9 July 2007 (Fig. 7), the REs of simulated versus monitored data for all stations were below 100% between 10:00 and 11:00. Between 11:00 and 12:00, the RE values for Stations 5 and 7 were the largest (125.8% and 189.4%, respectively). Between 12:00 and 13:00, the RE for Station 4 reached 1067.0%. Simulated DMF concentrations for Station 4 during other periods were also much higher than the concentrations recorded at other monitoring stations, which can be explained by that some factories close to Station 4 did not emit DMF on this particular monitoring day. The RE of Station 6 was the largest (323.7%) between 13:00 and 14:00. Wind direction of the monitoring period was north and the only nearby factory was downwind of Station 6, which may have resulted in a lower monitoring concentration. Overall, the REs between simulated and monitored data were below 50% at seven stations for 19 of the survey hours, accounting for 68% of the total monitoring points. REs in excess of 200% were recorded for two of the survey hours, accounting for 7% of total monitoring points.

On 10 July 2007 (Fig. 8), the REs of simulated versus monitored data for Stations 1 and 5 were greatest between 10:00 and 11:00 (171.1% and 388.4%, respectively). Between 11:00 and 12:00, the REs of these two stations were also the largest (178.8% and 353.4%, respectively). The nearby factories located to the east and north of Stations 1 and 5. The lower monitoring DMF concentrations between 10:00 and 12:00 may be attributed to relatively heavy winds (1.8 m/s) from the south direction. Between 12:00 and 13:00, Stations 3 and 4 had the largest REs (305.7% and 165.6%, respectively). Between 13:00 and 14:00, the REs of all stations were below 100% except for Station 6, which had an RE of 148.2%. Emission from the only factory to the south of the Station 6 and the lower wind speed (0.7 m/s) may result in the higher monitoring concentration of the station during this period. Overall, the REs of simulated versus monitored data for seven stations were below 50% for 12 of the survey hours, accounting for 43% of the total monitoring points. REs in excess of 200% were recorded for three of the survey hours,

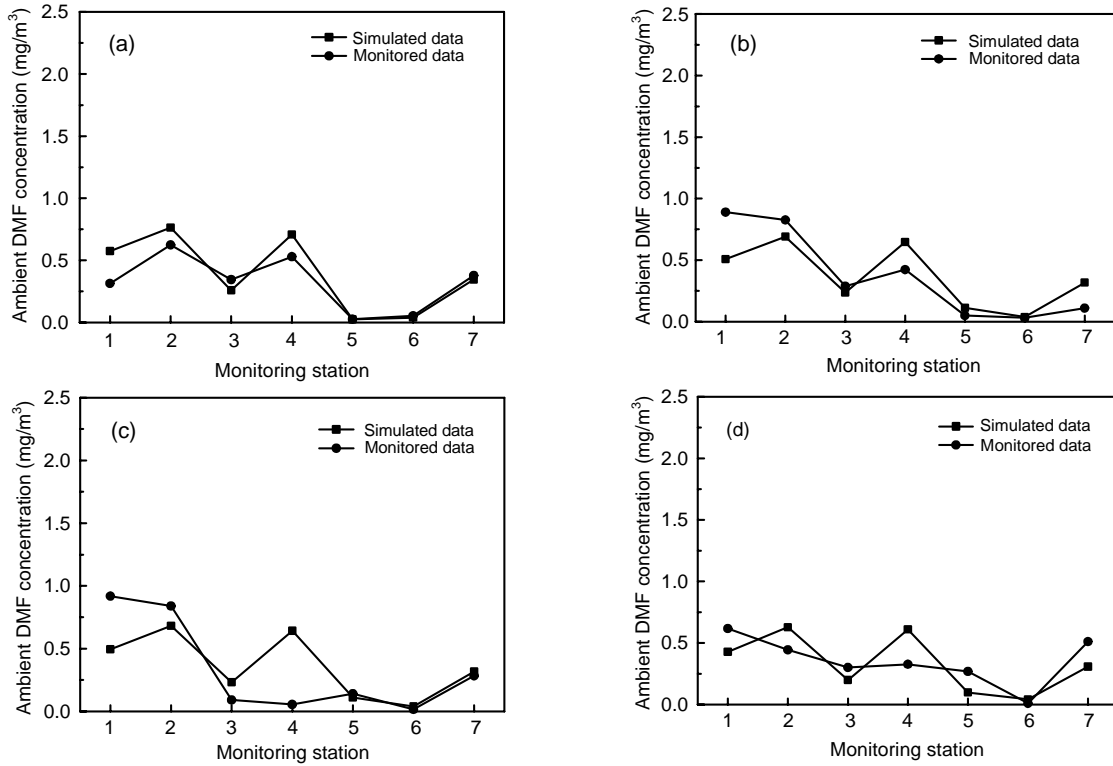


Fig. 7 Ambient DMF concentration for 9 July 2007 at 10:00–11:00 (a), 11:00–12:00 (b), 12:00–13:00 (c), and 13:00–14:00 (d)

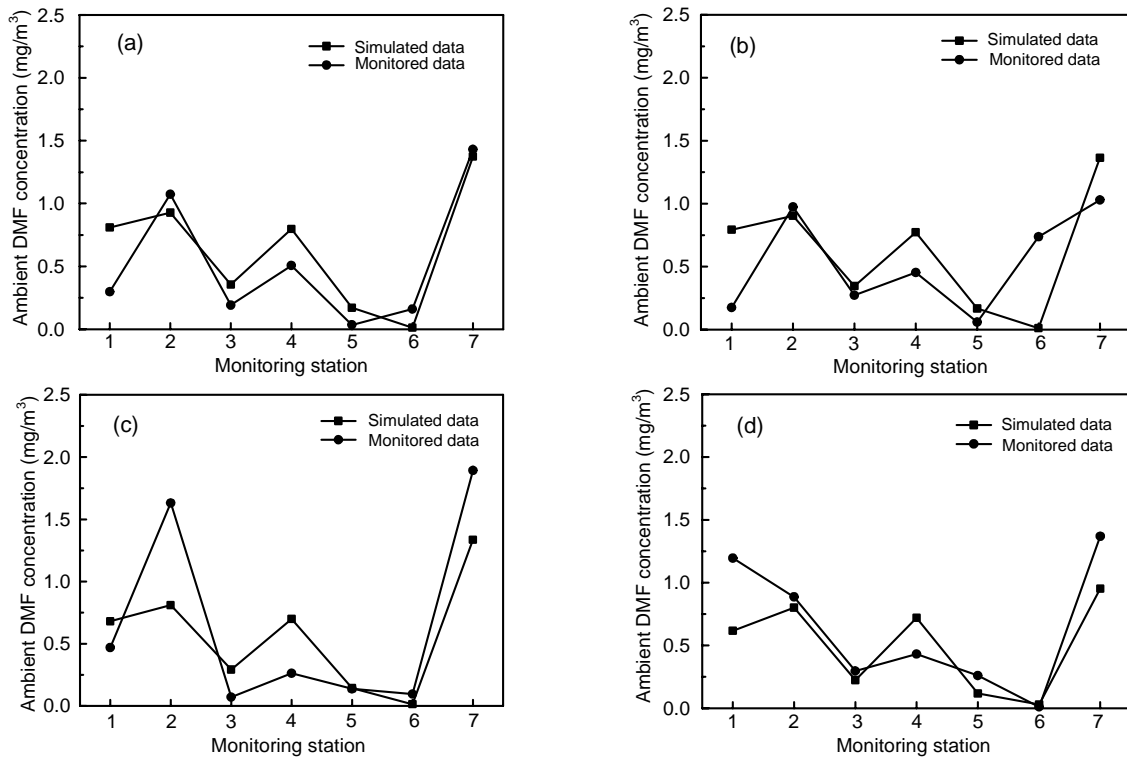


Fig. 8 Ambient DMF concentration for 10 July 2007 at 10:00–11:00 (a), 11:00–12:00 (b), 12:00–13:00 (c), and 13:00–14:00 (d)

accounting for 7% of the total monitoring points. Although larger REs were recorded at almost every station at some point during the monitoring period during this day, the tendency for the simulation to record variable DMF concentrations at different stations resulted in a close match with monitored DMF concentrations.

The total monitoring point results of these four days are 112 (i.e., 7 stations \times 4 h/d \times 4 d/station). Overall, the REs of simulated versus monitored data for seven stations were below 50% for 64 of the survey hours, accounting for 57% of the total monitoring points. Overall, REs exceeding 200% were recorded for eight of the survey hours, accounting for 7% of the total monitoring points. In total, 93% of the REs of simulated versus monitored data were within the range of 0.48%–189.4%. In order to evaluate the air pollutant dispersion Modelling results, it was important that the variety tendency of the simulated data closely matched that of the monitored data. Figs. 5–8 clearly showed that the simulated concentrations of all seven monitored stations produced similar results to the monitored concentrations.

4.4 Simulation of annual average DMF concentrations in 2006

Wind rose for the study area in 2006 is shown in Fig. 9. The prevailing wind direction in 2006 is north-north-east and the average wind speed is 3.0 m/s, which were in accordance with the representative meteorological conditions of the study area. Before 2003, DMF emissions of the study area kept growing with an increase of total production lines. Between 2003 and 2005, control measures were introduced to regulate DMF emissions, and total DMF emissions in the study area reduced gradually during these years. Since 2006, emissions of DMF stabilized at a relative low level (2.27×10^7 kg/yr). So, we selected the year of 2006 to simulate ambient DMF concentrations.

The simulated ambient DMF concentrations for 2006 of the approximate 100 km² modelled study area are shown in Fig. 10. In this figure, dark blue grids contain synthetic leather manufacturing factory production lines, accounting for 1.6% of the total grids. Red colored grids represent annual average ambient DMF concentrations of 4.0–9.75 mg/m³, green are of 1.0–4.0 mg/m³, yellow are of 0.4–1.0 mg/m³, and light blue colored are of less than 0.4 mg/m³, which

account for 0.15%, 2.5%, 7.02%, and 88.73% of the total grid area respectively. DMF concentrations were the highest at the north and southwest sections of the study area. This pattern can be attributed to the high density of nearby synthetic leather factories. The DMF fugitive emission threshold for industrial enterprises fence line in China is 0.4 mg/m³ (MEP-GAQSIQ, 2008). However, 11.27% of simulated average annual DMF concentrations of the study area recorded exceeded the threshold, even in the Longwan residential area. Available worldwide datasets with respect to ambient air DMF concentrations are limited. For example, in Lowell, Massachusetts, ambient DMF concentrations were above 0.15 mg/m³ of the industrial zone, and 0.024 mg/m³ in the residential

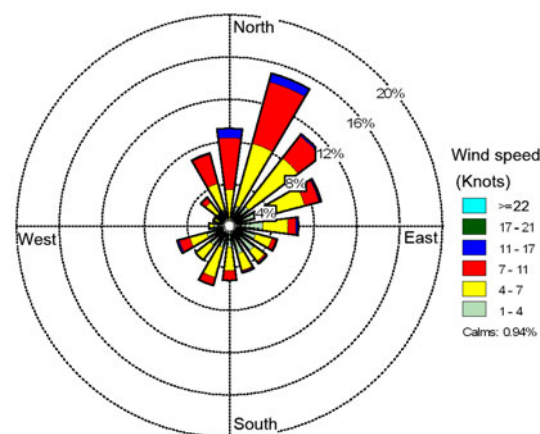


Fig. 9 Wind rose for the study area in 2006

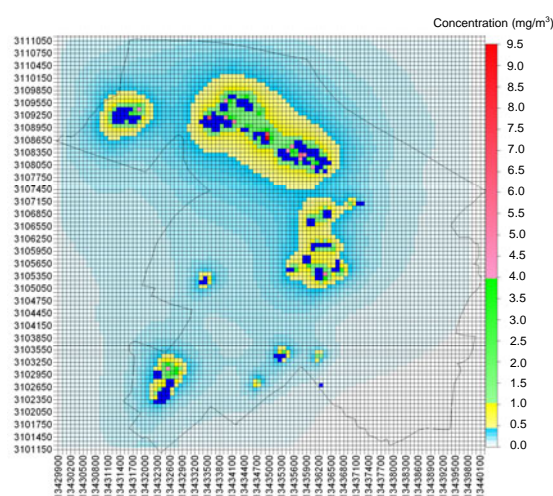


Fig. 10 Annual average ambient DMF concentration during 2006 using 100 m \times 100 m grids in the study area of the Longwan District of Wenzhou City, China

area (Amster *et al.*, 1983). In Germany, ambient air DMF concentrations of more than 5 pg/m^3 were recorded (CEPA, 1999). In Japan, ambient air DMF concentrations have been reported to be in the range of $0.1\text{--}10 \text{ mg/m}^3$ (Environment Agency Japan, 1996). However, given that the data from those studies were collected in the 1980s and 1990s, they may not represent current DMF concentrations.

4.5 Daily maximum simulated DMF concentrations in 2006

As DMF concentration was simulated for each grid, maximum daily DMF concentrations were the highest values of these concentrations everyday. As presented in Fig. 11, simulated maximum daily DMF concentrations for 2006 were in the range of $0.54\text{--}40.27 \text{ mg/m}^3$. The regulated exposure limit in China for DMF concentration in the air of a workplace is 10 mg/m^3 (MHPRC, 1979). For 71 d of 2006 (or 19.5% of the year), simulated maximum daily DMF concentrations were above 10 mg/m^3 . In other words, for one fifth of the year, DMF emissions would have been high enough to have a serious impact on human health in the Longwan District. For 107 d of 2006 (or 29% of the year), simulated maximum daily DMF concentrations were in the range of $4.0\text{--}10 \text{ mg/m}^3$. For 173 d of 2006 (or 47.4% of the year), simulated maximum daily DMF concentrations were in the range of $1.0\text{--}4.0 \text{ mg/m}^3$. For 15 d of 2006 (or 4.1% of the year), daily maximum simulated DMF concentrations were below 1.0 mg/m^3 .

4.6 Uncertainty analysis

Because data were modelled in this study, there was an expected degree of uncertainty derived from

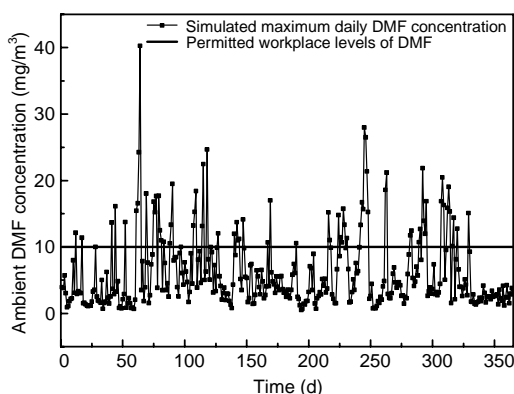


Fig. 11 Simulated maximum daily DMF concentrations versus permitted workplace levels in 2006

several parameters. First, the DMF emission inventories were established based on daily DMF consumption, disposal, and recycling in the manufacture of synthetic leather. Total DMF emissions in a year were closely related to the operating time of 54 synthetic leather factories. In our study, we set 210 d (24 h/d) as the average operating time for all factories in a given year. However, each factory in the study area had different operating times according to product demands, which ranged between 180–300 d of the year. Therefore, the use of 210 d as the average operating time may result in an uncertainty of DMF emission inventories. Second, during the investigation, the control facilities of some factories were not operational due to their being upgraded. This would have resulted in simulated DMF emissions and DMF concentrations that were higher than the monitored values. Third, because meteorological stations were not present in the immediate study area, the meteorological data used in our study were simulated using MM5. Onsite meteorological data were not measured during monitoring; instead, we used meteorological data from nearby meteorological stations to validate the simulated results of MM5. Comparison of simulated and monitored meteorological data indicated that the IOA and RMSE of wind speed were 0.84 and 0.1, respectively. The IOA and RMSE of wind direction were 0.83 and 63.2, respectively. Therefore, MM5 simulations performed well for wind speed, and the uncertainty of the simulation was mainly due to wind direction.

5 Conclusions

In this paper, the urban DMF emission inventories of 54 synthetic leather factories in a small-scale industrial area were established using the mass balance method. Annual and daily average concentrations of DMF in 2006 were simulated using AERMOD with receptor grids of $100 \text{ m} \times 100 \text{ m}$. Actual DMF concentrations recorded at seven DMF monitoring stations were compared with simulated results for the same timeframe. The results showed that the DMF emissions of wet and dry production lines were about 1.081×10^5 and $6.35 \times 10^4 \text{ kg/yr}$, respectively. Simulated annual average ambient DMF levels for the study area ranged from 0.048 to 9.75 mg/m^3 . The highest average simulated daily DMF concentrations

for grids outside of the workplace ranged from 0.54 to 40.27 mg/m³. Higher DMF concentrations were found in the vicinity of synthetic leather factories. The simulated concentrations of all seven monitoring stations produced similar results to the monitored ones. In total, 93% of the REs of simulated versus monitored data were within the range of 0.48%–189.4%. The variety tendencies of the simulated data closely matched those of the monitored data.

In the study area, DMF emission concentrations from chimney stacks and in the workplace of every factory were within the regulated emission limits. However, for 20% (71 d) of 2006, daily average ambient DMF concentrations in sections of the grid exceeded the workplace DMF concentration limit. Therefore, the maximum permitted emission of DMF from this industrial zone requires further regulation to protect the health of people in the Longwan District.

The DMF environmental capacity can be evaluated according to GIS-based DMF concentration simulations and the ambient DMF environmental quality standard. This information could be used to calculate the maximum DMF emissions within a specified region. Based on the geographic location of each factory, the emission quota of each factory could be established for environmental management.

Usually, high concentrations of air pollution occur in areas of close proximity to emission sources. As a result, air pollution in such areas is likely to be more harmful to humans, particularly in small-scale areas. Hence, it is vital to assess the health risk to humans posed by these sources of pollution (Venkatram *et al.*, 2004). GIS-based DMF concentration simulations using 100 m×100 m grids provide detailed DMF concentration distributions against which to conduct human health risk assessments and human exposure-response function research, particularly in areas where field monitoring data may not be available.

Acknowledgements

The authors would like to thank Longwan District Environmental Protection Bureau, Wenzhou Environment Monitoring Center, and Wenzhou Synthetic Leather Chamber of Commerce, Zhejiang, China, for their support to do this work.

References

- ADEC, 2009. ADEC Guidance re AERMET Geometric Means: How to Calculate the Geometric Mean Bowen Ratio and the Inverse-Distance Weighted Geometric Mean Surface Roughness Length in Alaska. Alaska Department of Environmental Conservation, Air Permits Programs, Alaska, USA.
- Amster, M.B., Hijazi, N., Chan, R., 1983. Real Time Monitoring of Low Level Air Contaminants from Hazardous Waste Sites. National Conference on Management of Uncontrolled Hazardous Waste Sites, Washington, DC, USA, p.98-99.
- An, X., Zuo, H., Chen, L., 2007. Atmospheric environmental capacity of SO₂ in winter over Lanzhou in China: a case study. *Advances in Atmospheric Sciences*, **24**(4):688-699. [doi:10.1007/s00376-007-0688-3]
- Calvert, G.M., Fajen, J.M., Hills, B.W., Halperin, W.E., 1990. Testicular cancer, dimethylformamide and leather tanneries. *The Lancet*, **336**(8725):1253-1254. [doi:10.1016/0140-6736(90)92870-N]
- CEPA, 1999. Priority Substances List Assessment Report: N, N-Dimethylformamide. Canadian Environmental Protection Act, Environment Canada, Health Canada, Ottawa, Canada.
- Cimorelli, A.J., Perry, S.G., Venkatram, A., Weil, J.C., Paine, R.J., Wilson, R.B., Lee, R.F., Peters, W.D., Brode, R.W., 2005. AERMOD: a dispersion model for industrial source applications Part I: general model formulation and boundary layer characterization. *Journal of Applied Meteorology*, **44**(5):682-693. [doi:10.1175/JAM2227.1]
- Coufal, C.D., Chavez, C., Niemeier, P.R., Carey, J.B., 2006. Nitrogen emissions from broilers measured by mass balance over eighteen consecutive flocks. *Poultry Science*, **85**(3):384-391.
- Environment Agency Japan, 1996. Chemicals in the Environment-Report on Environmental Survey and Wildlife Monitoring of Chemicals in F.Y. 1994. Environmental Health and Safety Division, Tokyo, Japan, p.119.
- Environment Canada, 1998. PSL2 Technical Report for N, N-dimethylformamide (1995–1996 data). Use Patterns Section, Chemicals Control Division, Commercial Chemicals Evaluation Branch, Quebec, Canada.
- Fang, C., Li, J., Meng, H., Yang, Y., Wang, J., 2008. Discussion of calculation to environmental capacity of atmosphere and gross control in the planning assessment. *Journal of Inner Mongolia Normal University (Natural Science Edition)*, **37**(4):550-553 (in Chinese).
- Goyal, P., Anand, S., Gera, B.S., 2006. Assimilative capacity and pollutant dispersion studies for Gangtok City. *Atmospheric Environment*, **40**(9):1671-1682. [doi:10.1016/j.atmosenv.2005.10.057]
- Grell, G.A., Dudhia, J., Stauffer, D.R., 1995. A Description of the Fifth-Generation Penn State/NCAR Mesoscale Model (MM5). National Center for Atmospheric Research, Boulder, Colorado, USA, p.122.

- Gunhan, T., Demir, V., Hancioglu, E., Hepbasli, A., 2005. Mathematical modelling of drying of bay leaves. *Energy Conversion and Management*, **46**(11-12):1667-1679. [doi:10.1016/j.enconman.2004.10.001]
- Han, Z., 2007. A regional air quality model: evaluation and simulation of O₃ and relevant gaseous species in East Asia during spring 2001. *Environmental Modelling & Software*, **22**(9):1328-1336. [doi:10.1016/j.envsoft.2006.07.007]
- Hansen, E., Meyer, O., 1990. Embryotoxicity and teratogenicity study in rats dosed epicutaneously with dimethylformamide (DMF). *Journal of Applied Toxicology*, **10**(5):333-338. [doi:10.1002/jat.2550100505]
- Horan, J.M., Finn, D.P., 2008. Sensitivity of air change rates in a naturally ventilated atrium space subject to variations in external wind speed and direction. *Energy and Buildings*, **40**(8):1577-1585. [10.1016/j.enbuild.2008.02.013]
- Howard, P.H., 1993. Handbook of Environmental Fate and Exposure Data for Organic Chemicals: Solvents 2, Volume 4. Lewis Publishers, Chelsea, Michigan, USA.
- Jilin Library, 1984. A Selection of Environmental Standards Abroad. Standards Press of China, Beijing, China (in Chinese).
- Klepeis, N.E., Gabel, E.B., Ott, W.R., Switzer, P., 2009. Outdoor air pollution in close proximity to a continuous point source. *Atmospheric Environment*, **43**(20):3155-3167. [doi:10.1016/j.atmosenv.2009.03.056]
- Krishna, T.V.B.P.S.R., Reddy, M.K., Reddy, R.C., Singh, R.N., 2004. Assimilative capacity and dispersion of pollutants due to industrial sources in Visakhapatnam bowl area. *Atmospheric Environment*, **38**(39):6775-6787. [doi:10.1016/j.atmosenv.2004.09.014]
- Lin, M., Lin, Y., 2002. The application of GIS to air quality analysis in Taichung City, Taiwan, ROC. *Environmental Modelling & Software*, **17**(1):11-19. [doi:10.1016/S1364-8152(01)00048-2]
- Matthias, V., Aulinger, A., Quante, M., 2008. Adapting CMAQ to investigate air pollution in North Sea coastal regions. *Environmental Modelling & Software*, **23**(3):356-368. [doi:10.1016/j.envsoft.2007.04.010]
- MEP-GAQSIQ, 2008. Emission Standard of Pollutants for Synthetic Leather and Artificial Leather Industry. Ministry of Environmental Protection of the People's Republic of China, General Administration of Quality Supervision, Inspection and Quarantine of the People's Republic of China. China Environmental Science Press, Beijing, China (in Chinese).
- MHPRC, 1979. Hygienic Standards for the Design of Industrial Enterprises, TJ36-79. Ministry of Health of the People's Republic of China (in Chinese).
- Özkaynak, H., Palma, T., Touma, J.S., Thurman, J., 2008. Modeling population exposures to outdoor sources of hazardous air pollutants. *Journal of Exposure Science and Environmental Epidemiology*, **18**(1):45-48. [doi:10.1038/sj.jes.7500612]
- Perry, S.G., Cimorelli, A.J., Paine, R.J., Brode, R.W., Weil, J.C., Venkatram, A., Wilson, R.B., Lee, R.F., Peters, W.D., 2005. AERMOD: A dispersion model for industrial source applications Part II: model performance against 17 field study databases. *Journal of Applied Meteorology*, **44**(5):694-708. [doi:10.1175/JAM2228.1]
- Samaali, M., Francois, S., Vinuesa, J., Ponche, J., 2007. A new tool for processing atmospheric emission inventories: technical aspects and application to the ESCOMPTE study area. *Environmental Modelling & Software*, **22**(12):1765-1774. [doi:10.1016/j.envsoft.2007.02.009]
- SEPA, 2003. Scheme for Environmental Capacity Estimation in the Urban Area. Ministry of Environmental Protection of the People's Republic of China. Available from <http://www.zhb.gov.cn/download/1084487068665.doc> (in Chinese) [Accessed on Oct. 25, 2010].
- Silverman, K.C., Tell, J.G., Sargent, E.V., Qiu, Z., 2007. Comparison of the industrial source complex and AERMOD dispersion models: case study for human health risk assessment. *Journal of the Air & Waste Management Association*, **57**(12):1439-1446. [doi:10.3155/1047-3289.57.12.1439]
- Sokhi, R.S., San Jose, R., Kitwiroon, N., Fragkoua, E., Perez, J.L., Middleton, D.R., 2006. Prediction of ozone levels in London using the MM5-CMAQ modeling system. *Environmental Modelling & Software*, **21**(4):566-576. [doi:10.1016/j.envsoft.2004.07.016]
- Spicer, C.W., Buxton, B.E., Holdren, M.W., Smith, D.L., Kelly, T.J., Rust, S.W., Pate, A.D., Sverdrup, G.M., Chuang, J.C., 1996. Variability of hazardous air pollutants in an urban area. *Atmospheric Environment*, **30**(20):3443-3456. [doi:10.1016/1352-2310(95)00200-6]
- Titov, M., Sturman, A.P., Zawar-Reza, P., 2007. Application of MM5 and CAMx4 to local scale dispersion of particulate matter for the city of Christchurch, New Zealand. *Atmospheric Environment*, **41**(2):327-338. [doi:10.1016/j.atmosenv.2006.08.012]
- US EPA, 2004a. User's Guide for the AMS/EPA Regulatory Model: AERMOD. Office of Air Quality Planning and Standards, Research Triangle Park, US Environmental Protection Agency, North Carolina, USA.
- US EPA, 2004b. User's Guide for the AERMOD Meteorological Preprocessor (AERMET). Office of Air Quality Planning and Standards, Research Triangle Park, US Environmental Protection Agency, North Carolina, USA.
- US EPA, 2008. AERSURFACE User's Guide. Office of Air Quality Planning and Standards, US Environmental Protection Agency, North Carolina, USA.
- Venkatram, A., Isakov, V., Yuan, J., Pankratz, D., 2004. Modeling dispersion at distances of meters from urban sources. *Atmospheric Environment*, **38**(28):4633-4641. [doi:10.1016/j.atmosenv.2004.05.018]
- Wang, S., Shih T., Huang, Y., Chueh, M., Chou, J., Chang, H., 2006. Evaluation of the effectiveness of personal protective equipment against occupational exposure to N, N-dimethylformamide. *Journal of Hazardous Materials*, **138**(3):518-525. [doi:10.1016/j.jhazmat.2006.05.072]
- Willmott, C.J., 1981. On the validation of models. *Physical Geography*, **2**(2):184-194.

- Yang, X., Gao, Q., Qu, J., Jiang, Z., 1999. The exploration and initial assessment of total amount control method for SO₂ emission in China. *Research of Environmental Science*, **12**(6):17-20 (in Chinese).
- Zawar-Reza, P., Kingham, S., Pearce, J., 2005. Evaluation of a year-long dispersion modelling of PM₁₀ using the mesoscale model TAPM for Christchurch, New Zealand. *Science of the Total Environment*, **349**(1-3):249-259. [doi:10.1016/j.scitotenv.2005.01.037]
- Zhang, Q., 2007. Atmospheric Environmental Capacity Calculation of DMF and Dimethylamine from Synthetic Leather Plants in Longwan District of Wenzhou City. Project Report, Wenzhou, China (in Chinese).
- Zhang, Q., Wei, Y., Tian, W., Yang, K., 2008. GIS based emission inventories of urban-scale: a case study of Hangzhou, China. *Atmospheric Environment*, **42**(20): 5150-5165. [doi:10.1016/j.atmosenv.2008.02.012]
- Zhou, Y., Levy, J.I., Hammitt, J.K., Evans, J.S., 2003. Estimating population exposure to power plant emissions using CALPUFF: a case study in Beijing, China. *Atmospheric Environment*, **37**(6):815-826. [doi:10.1016/S1352-2310(02)00937-8]

